Design and Optimization of a 10 nH Square-Spiral Inductor for Si RF Ics.

For the degree of Master of Science in Electrical and Computer Engineering.

University of North Carolina at Charlotte.

Student: Tuan Huu Bui.
Advisor: Dr. Thomas P. Weldon.
Date completed: 10/27/1999.

Contents

Abstract

Nowadays, as the demand for wireless communication continues to expand, the need for high quality (Q) inductors for high-level integration of RF circuit, in order to reduce cost, has become more important. Recently, many research activities have been focused on the design, model and optimization of spiral inductors on silicon substrate. However, most of the reported Q of spiral inductors is limited to below 10 at giga hertz range. In this project, the Si IC spiral inductor is analyzed using electromagnetic analysis. With appropriate approximations, the calculations are reduced to electrostatic and magnetostatic calculations. The important effects of substrate loss are included in the design. Classical circuit analysis and network analysis techniques are used to derive two-port parameters from the circuits. This analysis is applied to traditional square inductor structure.

Introduction

Modern silicon integrated circuits are finding wide application in the GHz frequency range. The CMOS and BiCMOS processes provide high f_T transistors allowing Si RF-ICs to compete with GaAs ICs in the important low GHz frequency ranges. However, the lossy Si substrate makes the design of high Q reactive components difficult. Despite this difficulty, the low cost of Si IC fabrication over GaAs IC fabrication and the potential for integration with baseband circuits makes Si the process of choice in many RF IC applications.

The demands placed on wireless communication circuits include low supply voltage, low cost, low power dissipation, low noise, high frequency of operation and low distortion. These design requirements cannot be met satisfactorily in many cases without the use of RF inductors. Hence, there is a greatly incentive design, optimize, and model spiral inductors fabricated on Si substrates. Typical applications of on-chip inductors include low loss inductors for input matching of low noise amplifiers, inductively loaded pre-amplifiers, output matching networks for high efficiency switch-mode power amplifiers, and high Q tank circuits for low phase noise voltage control oscillators. The design has included higher conductivity metal layers to reduce the loss resistance of inductor. The use of multi-metal layers to increase the effective thickness of the spiral inductor and thereby reduce loss. The connection of multi-metal layer spirals in series to reduce the area of the inductors, the low-loss substrates to reduce losses in the substrate at high frequency, and thick oxide or floating inductors to isolate the inductor from the lossy substrate.

In an analysis approach is presented where an equivalent circuit for each segment of the spiral is calculated and the inductor is considered as an interconnection of such segments. The approach is limited, though, as many important effects are not included. For instance, non-uniform current distribution due to skin and proximity effects within each segment is not considered. In addition, the impedance to substrate is calculated

using a 2-dimensional approach, making it difficult to apply to arbitrary structures or to coupled inductors.

Most past researchers have used measurement results on previously built inductors to construct models. While this technique is most practical, it does not allow the possibility of optimization nor does it allow the circuit designer freedom to choose parameters such as inductance, capacitance and Q. Otherwise researchers have used commercial 3D electromagnetic simulators to design and analyze inductors. While this approach is accurate, it can be computationally very expensive and time-consuming. This design presents an accurate and computationally efficient approach to overcome the requirement.

Project Overview

Since square spiral inductors are the most common in Si RF IC's. So, the target of this project is to design a 10nH square spiral inductor with high quality factor (Q). The solution is to find the number of turns and all dimensions of the square spiral inductor. Another importance part of the spiral inductor is the substrate. The quality factor of spiral inductor depends on the materials that constructed from substrate. So, another problem is to find the materials to design that substrate that produces a high quality factor and low cost.

1. Background

The inductance of a planar spiral square inductor can be calculated according to the Greenhouse theory. Basically, the spiral square inductor is split up into sections consisting of straight conductors, and the self-inductance of the sections is calculated and summed up. Beside the consideration of the self-inductance of each straight conductor, the mutual inductance (positive or negative) between parallel segments needs to be included for the calculation of the overall inductance.

1.1 Self-Inductance

The self-inductance for a straight conductor is,

$$L = 0.002l\left[\ln\left(\frac{2l}{GMD}\right) - 1.25 + \frac{AMD}{l} + \left(\frac{\mu}{4}\right)T\right] \qquad (1)$$

Where L is the self-inductance in microhenries, l is the conductor length in cm, GMD and AMD represent the geometric and arithmetic mean distance, respectively, of the conductor cross section, μ is the conductor permeability, and T is the frequency-correction parameter.

The geometric mean distance (GMD) between two conductors is the distance between two infinitely thin imaginary filaments whose mutual inductance is equal to the mutual

inductance between the two original conductors (fig. 1b). The GMD is equal to 0.44705 times a side in the case of a square cross section.

The arithmetic mean distance (AMD) is the average of all the distances between the points of one conductor and the points of another. For a single conductor, the arithmetic mean distance is the average of all possible distances within the cross section.

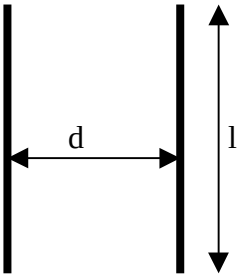

Fig. 1a. Layout of current filaments.

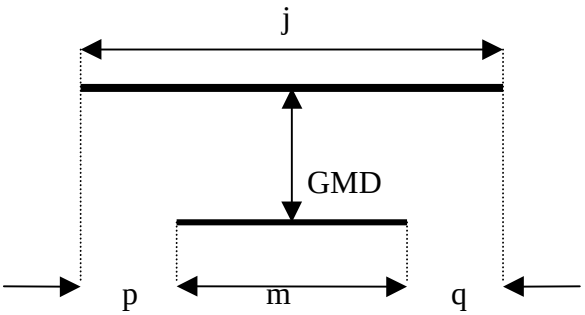

Fig. 1b. Two parallel-filament geometry.

If we usr the top layer of metal for the layout of the spiral inductor, we can consider it as a thin-film inductor with rectangular cross section and equation (1) takes the form

$$L = 0.002l\left[\ln\left(\frac{2l}{a+b}\right) + 0.50049 + \frac{a+b}{3l}\right] \qquad (2)$$

Where a, b are the rectangular dimension of the cross section. The magnetic permeability μ is 1, and the skin-depth phenomenon has little effect on thin film, T should be considered to have a value of 1 for microwave frequencies.

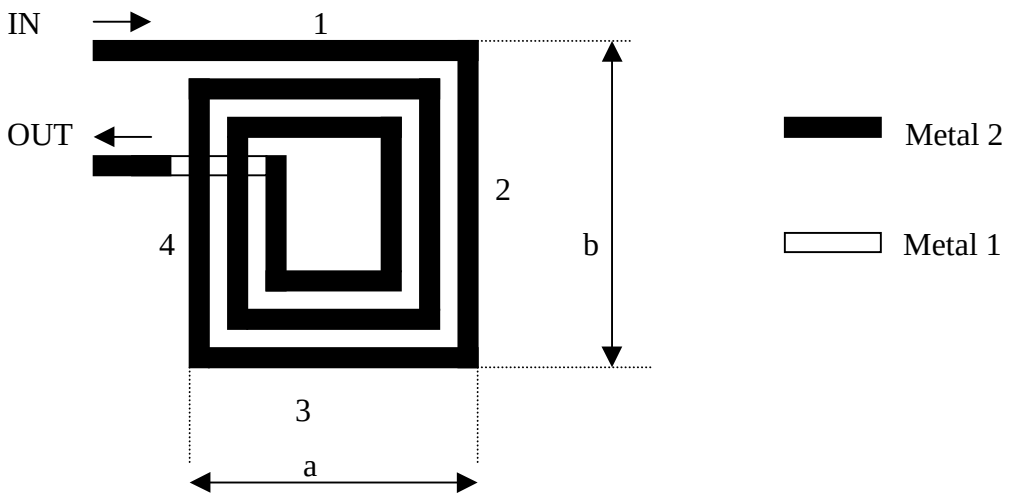

Fig. 2. Layout of a typical rectangular spiral inductor.

Table.1
Variation in Frequency-Correction Parameter T for
Thin Films and Microwave Frequencies.

Value of T	Film Thickness	Frequency
0.9974	10,000 angstroms	10 gigahertz
0.9986	0.0025 millimeter (0.1 mil)	1 gigahertz
0.9095	0.0075 millimeter (0.7 mil)	1 gigahertz

1.2 Mutual inductance

In the case of an L-shaped thin-film inductor, total inductance is equal to the sum of the self-inductance of the two straight segments, and less than the inductance of a single straight track of equal length. In the case of a rectangular of square planar coil, straight conductor segments are parallel to other straight conductor segments, and the mutual inductance between these parallel tracks contributes to the total inductance of the coil.

Figure.2 shows the top view of a 3-turn spiral inductor. For a typical process with two layers of metal, the top layer is used for forming the spiral inductor and the bottom layer for routing the inner turn outward. As the metal layer is separated from the substrate with an oxide layer, so the top layer is used for the inductor layout so as to increase the oxide thickness from the ground so that the substrate effect will be reduced and the self-resonant frequency improved. Secondly, the top layer has a thicker layer of metal of metal which help to reduce both the dc and high frequency resistance so that factor of the inductor can be improved.

The inductance of the spiral in Fig.1 is equal to the sum of the self-inductance for each segment in the coil plus the mutual inductance, which are determined by the geometry and the phase relationship between the current carried by those lines. Figure 3 shows the model of two straight conductors carrying in-phase or out-of-phase current. There is a mutual inductance of M between the two conductors. For in-phase current such

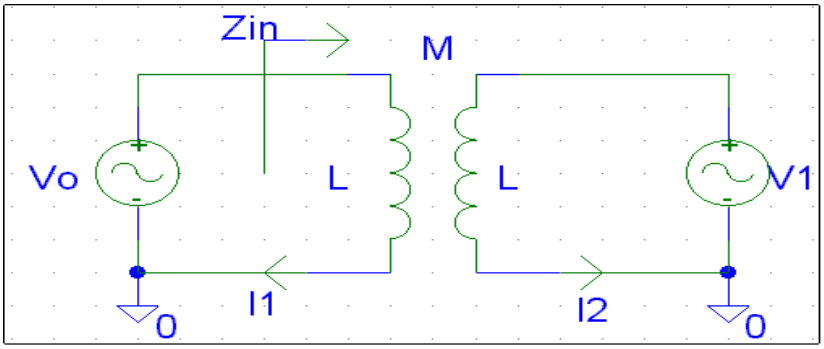

Fig.3 Modeling of two conductors carrying in-phase and out-of-phase current

as the current in segment 1 and 5 of the inductor in figure 2, two equations (shown below) govern the voltages and currents in the two conductors,

$$V_0 = I_1(jw\omega L) + I_2(jw\omega LM) \quad (3)$$

$$V_1 = I_2(jw\omega L) + I_1(jw\omega LM) \quad (4)$$

and for in phase current ($V_1 = V_2$). After manipulation of the equation (3) and (4), one can calculate that the impedance Z_{in} of segment 1 is,

$$Z_{in} = jw\omega(L+M) \tag{5}$$

which means the inductance of the conductor increases by M, and M is the mutual inductance between the two conductors. So, parallel currents travelling in phase can contribute positive mutual components of inductance. For the case of out-of-phase current, such as current in segment 5 and 7, the calculation of the impedance Z_{in} is almost the same but now $V_1 = -V_0$ and will contribute negative mutual components of inductance. Thus the inductance of a conductor can be expressed as,

$$L = L_{self} \pm M \tag{6}$$

The mutual inductance between two parallel conductors is a function of the length of the conductors and of the geometric distance between them. In general,

$$M = 2lQ \tag{7}$$

where M is the mutual inductance in nH, l is the conductor length in cm, and Q is the mutual inductance parameter calculated from the equation

$$Q = \ln\left[\frac{1}{GMD} + \sqrt{1+\frac{l^2}{(GMD)^2}}\right] - \sqrt{1+\frac{(GMD)^2}{l^2}} + \frac{GMD}{l} \tag{8}$$

where GMD, the geometric mean distance between the two conductors, is approximately equal to the distance between the track center. The exact value of the GMD is,

$$\ln GMD = \ln d - \left[\frac{1}{12\left(\frac{d}{w}\right)^2} + \frac{1}{60\left(\frac{d}{w}\right)^4} + \frac{1}{168\left(\frac{d}{w}\right)^6} + \frac{1}{360\left(\frac{d}{w}\right)^8} + \frac{1}{660\left(\frac{d}{w}\right)10} + \ldots\right] \tag{9}$$

where d is the center to the center separation between the conductors, and w is the width of the conductors.

For two parallel conductors with lengths of j and m (Fig.1b), the total mutual inductance can be represented by

$$2M_{j,m} = (M_{m+p} + M_{m+q}) - (M_p + M_q) \quad (10)$$

and the individual M terms are calculated using equation (7) and the lengths corresponding to the subscript, which is

$$M_{m+p} = 2l_{m+p} Q_{m+p} = 2(m + p)Q_{m+p} \quad (11)$$

where Q_{m+p} is the mutual-inductance parameter Q for GMD/(m + p). The total inductance of the spiral in figure.2, which neglects the extra routing segments, is the sum of the self-inductances of each of the straight segments (L_1..L_n) plus all the mutual inductances between the segments, which is

$$L_T = L_0 + M_+ + M_- \quad (12)$$

where L_T is the total inductance, L_0 is the sum of the self-inductances of all straight segments, M_+ is the sum of the positive mutual inductances and M_- is the sum of the negative mutual inductances.

1.3 Skin depth effect

The resistance of a metal segment will increase as frequency rises due to the skin depth effect. The skin depth of metal is shown below,

$$\delta = \sqrt{\frac{\rho}{\pi \mu f}} \quad (13)$$

where δ is the skin depth, ρ is the frequency and μ is the permeability of free space, $4\pi\times10^{7}$. The skin resistance R_S is,

$$R_S = \frac{\rho}{\delta} \tag{14}$$

For aluminum, the skin depth is approximately 1.2μm at 5GHz, roughly the thickness of metal lines in IC fabrication process. This implies that the series resistance of the spiral would not deviated much from its DC value up to 5GHz. For this reason, the skin depth effect will be ignored in the design.

1.4 Inductor Quality Factor

The quality of an inductor is measured by its Q, which is defined as

$$Q = 2\pi \frac{\text{energy stored}}{\text{energy loss in one oscillation cycle}} \tag{15}$$

For an inductor, only the energy stored in the magnetic field is of interest. Any energy stored in the inductor's electric field, because of some inevitable parasitic capacitances in a real inductor, is a loss. Hence, Q is proportional to the net magnetic energy stored, which is equal to the difference between the peak magnetic and electric energies. An inductor is at self-resonance when the peak magnetic and electric energies are equal. Therefore, Q vanishes to zero at the self-resonance frequency. Above the self-resonance frequency, no net magnetic energy is available from an inductor to any external circuit. To be more detail, the inductor Q can be defined as,

$$Q = 2\pi \frac{\text{peak magnetic energy - peak electric energy}}{\text{energy loss in one oscillation cycle}} = \frac{R}{\omega L}\left[1-\left(\frac{\omega}{\omega_0}\right)^2\right] \tag{16}$$

which equals zero at $\omega = \omega_0$, and is less than zero beyond ω_0. In terms of impedance, Q is equal to the ratio of the imaginary to the real part of the circuit impedance. The circuit impedance is inductive below ω_0 and capacitive above ω_0.

In some simple RF circuits, Q can be found by equations

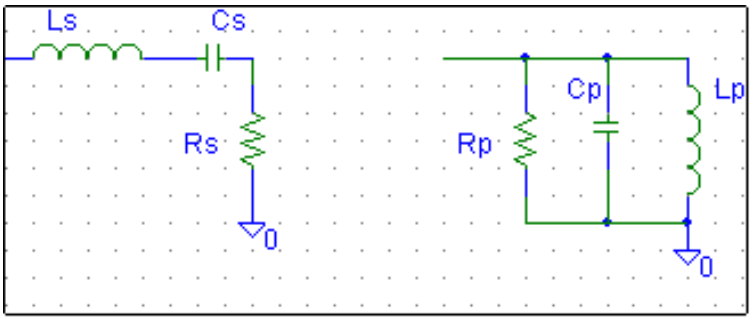

Fig. 4 The serial and parallel circuit models

For parallel circuit

$$Q = \frac{Rp}{|Xp|} \tag{17}$$

and for serial circuit

$$Q = \frac{|Xs|}{Rs} \tag{18}$$

2. Physical Inductor Model

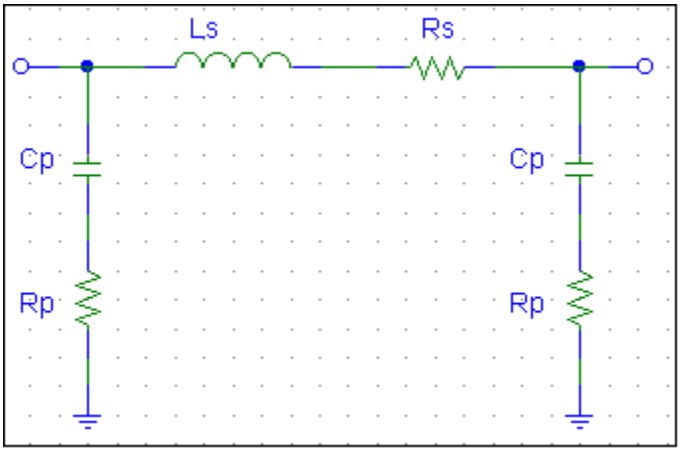

Fig. 5 Equivalent circuit of a spiral inductor

Each segment of the inductor is modeled with a two-port network consisting of elements, as shown in figure 5. Two coupled micro-strips in a typical silicon process are drawn in figure 6. The geometry characteristics of interest are the track width w of the spiral; the distance between two adjacent parallel tracks s and the height of the metal track t. the height of the Si substrate and the SiO_2 insulator are h_{Si} and h_{SiO_2} respectively. The main elements of the two-port are the series inductance L_S, the resistance R_S of the segment and the capacitors C_p formed by the insulating SiO_2 between the inductor and the Si substrate. All equations are shown below

$$R_S = R_{sh}\frac{l}{w} \tag{19}$$

$$C_p = \varepsilon_o \varepsilon_r \frac{w}{h_{Si}} \tag{20}$$

$$R_{sub} = \rho_{Si}\frac{l}{wh_{Si}} \tag{21}$$

where R_{sh} is the sheet resistance of the metal track. All lengths are in cm, while inductance is in nH and capacitance in pF. In this circuit, L_S models the self and mutual inductances in the second-metal segments, R_S is the accumulated sheet resistance, C_P models the parasitic capacitance from the second-metal layer to the substrate, and R_P represents the resistance of the conductive Si substrate. If one side of the inductor is grounded, the self-resonant frequency of the spiral inductor can be derived from the equivalent circuit. It is approximately equal to

$$\omega_R = \frac{1}{\sqrt{L_S C_P}}\left[\frac{1-R_S^2\left(\frac{C_P}{L_S}\right)}{1-R_P^2\left(\frac{C_P}{L_S}\right)}\right]^{\frac{1}{2}} \tag{22}$$

Beyond the resonant frequency, the inductor becomes capacitive. Frequency ω_R is limited by C_P, which is inversely proportional to the oxide thickness between the second-metal layer and the substrate.

3. The Design of 10nH Square Spiral Inductor

This design is based on the background and equations that are introduced from previous sections. In this design, the 2μm-process will be used to fabricate the chip. So, all the design specifications have met for the process. There are a lot of math equations involved the project. To simplify the problem, MathCad program was used to approach the result. That program is shown below.

$t := 0.0001\ \text{cm}$ $s := 0.0004\ \text{cm}$ $w := 0.0006\ \text{cm}$ $l_1 := 0.0213\ \text{cm}$ $N := 7$ (inputs)

$k := 4 \cdot N$

$r := 2..(2 \cdot N)$

$l_2 := l_1$ $l_3 := l_1$

$l_{2 \cdot r} := l_2 - (r - 1) \cdot (w + s)$

$l_{2 \cdot r - 1} := l_1 - (r - 2) \cdot (w + s)$

$$\text{length} := \sum_{y=1}^{k} l_y$$

$l_1 = 0.0213$

$l_2 = 0.0213$

$l_3 = 0.0213$ $l_4 = 0.0203$ cm

$\text{length} = 0.4274$ cm

$y := 1..k$

$$L_y := 0.002 l_y \cdot \left[\ln\left[2 \cdot \frac{l_y}{(w + t)} \right] + 0.50049 + \left(\frac{w + t}{3 \cdot l_y} \right) \right]$$

$$L_0 := \sum_{y=1}^{k} 10^3 \cdot L_y$$

$$L_0 = 3.6982 \quad \text{nH}$$

$$GMD1 := \left| \begin{array}{l} \text{for } j \in 1..k \\ \quad \text{for } n \in 1..N \\ \quad\quad t_{j,(j+4\cdot n)} \leftarrow e^{\ln(n\cdot(s+w)) - \left[1 + \frac{1}{12\cdot\left[\frac{n\cdot(s+w)}{w}\right]^2} + \frac{1}{60\cdot\left[\frac{n\cdot(s+w)}{w}\right]^4} + \frac{1}{168\cdot\left[\frac{n\cdot(s+w)}{w}\right]^6}\right]} \quad \text{if } (j+4\cdot n) \le k \\ \quad\quad 0 \quad \text{otherwise} \\ t \end{array} \right.$$

$$M1j := \left| \begin{array}{l} sum1 \leftarrow 0 \\ \text{for } j \in 1..k \\ \quad \text{for } n \in 1..N \\ \quad\quad sum1 \leftarrow sum1 + 2\cdot l_j \cdot \left[\left[\ln\left[\frac{l_j}{GMD1_{j,(j+4\cdot n)}} + \left[1 + \left[\frac{l_j}{GMD1_{j,(j+4\cdot n)}}\right]^2\right]^{0.5}\right] - \left[1 + \left[\frac{GMD1_{j,(j+4\cdot n)}}{l_j}\right]^2\right]^{0.5}\right] + \frac{GMD1_{j,(j+4\cdot n)}}{l_j}\right] \quad \text{if } (j+4\cdot n) \le k \\ \quad\quad 0 \quad \text{otherwise} \\ sum1 \end{array} \right.$$

$$M1m := \left| \begin{array}{l} sum1m \leftarrow 0 \\ \text{for } j \in 1..k \\ \quad \text{for } n \in 1..N \\ \quad\quad sum1m \leftarrow sum1m + 2\cdot l_{j+4\cdot n} \cdot \left[\left[\ln\left[\frac{l_{j+4\cdot n}}{GMD1_{j,(j+4\cdot n)}} + \left[1 + \left[\frac{l_{j+4\cdot n}}{GMD1_{j,(j+4\cdot n)}}\right]^2\right]^{0.5}\right] - \left[1 + \left[\frac{GMD1_{j,(j+4\cdot n)}}{l_{j+4\cdot n}}\right]^2\right]^{0.5}\right] + \frac{GMD1_{j,(j+4\cdot n)}}{l_{j+4\cdot n}}\right] \\ \quad\quad 0 \quad \text{otherwise} \\ sum1m \end{array} \right.$$

if $(j+4\cdot n) \le k$

$$M1p := \left| \begin{array}{l} sum1p \leftarrow 0 \\ \text{for } j \in 1..k \\ \quad \text{for } n \in 1..N \\ \quad\quad \left| \begin{array}{l} sum1p \leftarrow sum1p + 2\cdot\left(l_j - l_{j+4\cdot n}\right)\cdot\left[\left[\ln\left[\frac{l_j - l_{j+4\cdot n}}{GMD1_{j,(j+4\cdot n)}} + \left[1+\left[\frac{l_j - l_{j+4\cdot n}}{GMD1_{j,(j+4\cdot n)}}\right]^2\right]^{0.5}\right] - \left[1+\left[\frac{GMD1_{j,(j+4\cdot n)}}{l_j - l_{j+4\cdot n}}\right]^2\right]^{0.5}\right] + \frac{GMD1_{j,(j+4\cdot n)}}{l_j - l_{j+4\cdot n}}\right] \\ 0 \quad \text{otherwise} \end{array} \right. \\ sum1p \end{array} \right.$$

$$\text{if } (j+4\cdot n) \le k$$

$$M1 := M1j + M1m - M1p$$

$$M1 := 12.5647 \quad nH$$

$$GMD2 := \left| \begin{array}{l} \text{for } j \in 1..k \\ \quad \text{for } n \in 1..N \\ \quad\quad \left| \begin{array}{l} u_{j,(j+4\cdot n-2)} \leftarrow e^{\ln\left[l_{j+1} - n\cdot(s+w)\right] - \left[1 + \frac{1}{12\cdot\left[\frac{l_{j+1} - n\cdot(s+w)}{w}\right]^2} + \frac{1}{60\cdot\left[\frac{l_{j+1} - n\cdot(w+s)}{w}\right]^4} + \frac{1}{168\cdot\left[\frac{l_{j+1} - n\cdot(s+w)}{w}\right]^6}\right]} \quad \text{if } (j+4\cdot n-2) \le k \\ 0 \quad \text{otherwise} \end{array} \right. \\ u \end{array} \right.$$

$$M2m := \left| \begin{array}{l} sum2m \leftarrow 0 \\ \text{for } j \in 1..k \\ \quad \text{for } n \in 1..N \\ \quad\quad \left| \begin{array}{l} sum2m \leftarrow sum2m + \left(2\cdot l_{j+4\cdot n-2}\right)\left[\ln\left[\frac{l_{j+4\cdot n-2}}{GMD2_{j,(j+4\cdot n-2)}} + \left[1+\left[\frac{l_{j+4\cdot n-2}}{GMD2_{j,(j+4\cdot n-2)}}\right]^2\right]^{0.5}\right] - \left[1+\left[\frac{GMD2_{j,(j+4\cdot n-2)}}{l_{j+4\cdot n-2}}\right]^2\right]^{0.5}\right] \\ 0 \quad \text{otherwise} \end{array} \right. \\ sum2m \end{array} \right.$$

$$+ \frac{GMD2_{j,(j+4\cdot n-2)}}{l_{j+4\cdot n-2}} \quad \text{if} \quad (j+4\cdot n-2) \le k$$

$$
\begin{aligned}
&2p := \left|\begin{array}{l}
\text{sum2p} \leftarrow 0 \\
\text{for } j \in 1..k \\
\quad \text{for } n \in 1..N \\
\quad\quad \left|\begin{array}{l}
\left[\text{sum2p} \leftarrow \text{sum2p} + 2\cdot\left(l_j - l_{j+4\cdot n-2}\right)\cdot\left[\ln\left[\frac{l_j - l_{j+4\cdot n-2}}{2\cdot GMD2_{j,(j+4\cdot n-2)}} + \left[1+\left[\frac{l_j - l_{j+4\cdot n-2}}{2\cdot GMD2_{j,(j+4\cdot n-2)}}\right]^2\right]^{0.5}\right] - \left[1+\left[\frac{2\cdot GMD2_{j,(j+4\cdot n-2)}}{l_j - l_{j+4\cdot n-2}}\right]^2\right]^{0.5}\right]\right] \\
0 \quad \text{otherwise}
\end{array}\right. \\
\text{sum2p}
\end{array}\right. \\
&\qquad\qquad \blacksquare + \frac{2\cdot GMD2_{j,(j+4\cdot n-2)}}{l_{j+4\cdot n-2}} \text{ if } (j+4\cdot n-2) \le k
\end{aligned}
$$

$$
\begin{aligned}
&2j := \left|\begin{array}{l}
\text{sum2} \leftarrow 0 \\
\text{for } j \in 1..k \\
\quad \text{for } n \in 1..N \\
\quad\quad \left|\begin{array}{l}
\left[\text{sum2} \leftarrow \text{sum2} + 2\cdot l_j\cdot\left[\left[\ln\left[\frac{l_j}{GMD2_{j,(j+4\cdot n-2)}} + \left[1+\left[\frac{l_j}{GMD2_{j,(j+4\cdot n-2)}}\right]^2\right]^{0.5}\right] - \left[1+\left[\frac{GMD2_{j,(j+4\cdot n-2)}}{l_j}\right]^2\right]^{0.5}\right] + \frac{GMD2_{j,(j+4\cdot n-2)}}{l_j}\right]\right] \\
0 \quad \text{otherwise}
\end{array}\right. \\
\text{sum2}
\end{array}\right. \\
&\qquad\qquad \text{if } (j+4\cdot n-2) \le k
\end{aligned}
$$

$M2 := M2j + M2m - M2p$

$M2 = 6.2397 \quad nH$

$Ltt := L_0 + M1 - M2$

$Ltt = 10.0232 \quad nH$

$Rsh := 0.03 \ \frac{ohm}{sq} \qquad \varepsilon r := 3.9 \qquad \varepsilon o := \frac{10^{-9}}{36 \cdot \pi} \qquad \rho si := 0.1 \quad ohm \cdot cm$

$hsi := 0.03 \quad cm \qquad hsio := 0.0003 \quad cm$

$Rsub_y := \frac{\rho si \cdot l_y}{w \cdot hsi}$

$Rp := \sum_{y=1}^{k} Rsub_y$

$Rs := \frac{length}{w} \cdot Rsh$

$Rs = 21.37 \quad ohms$

$Rp = 2.3744 \cdot 10^{3} \quad ohms$

$Cp := \varepsilon o \cdot \varepsilon r \cdot \frac{w}{hsi}$

$Cp = 6.8967 \cdot 10^{-13} \quad F$

The results from MathCad are shown in the table.2 and table.3 below

Table.2

The geometric values of square-spiral inductor from Mathcad.

Thickness t (μm)	Space between segments s (μm)	Width W (μm)	Outer length l_1 (μm)	Number of turns	Total Inductance L (nH)
1	4	6	213	7	10.02

The $5\frac{1}{4}$ turns that means square spiral inductor has 21 segments, which shown in figure

Table.3

R_S (ohms)	R_P (ohms)	C_P (pF)	ω_R (rad/s)
21.37	2.1K	0.7	3.8×10^5

The two-port circuit of the 10nH square-spiral inductor can be represented as figure 6.

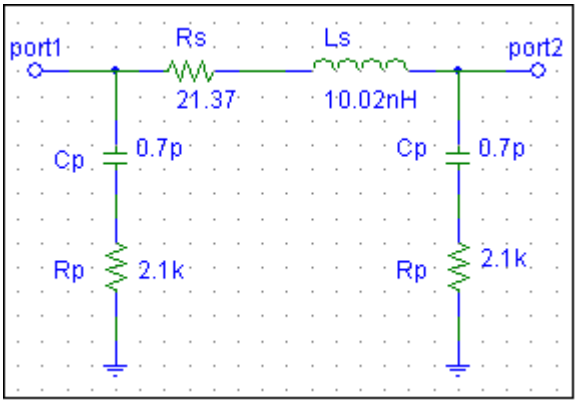

Fig.6: Equivalent circuit of the 10nH Square-Spiral Inductor.

The S_{11}-parameter of the two-port network above is plotted on Smith chart, which is shown in attachment. Finally, The physical of the spiral inductor will be fabricated as the figure.7a and figure.7b in attachment.

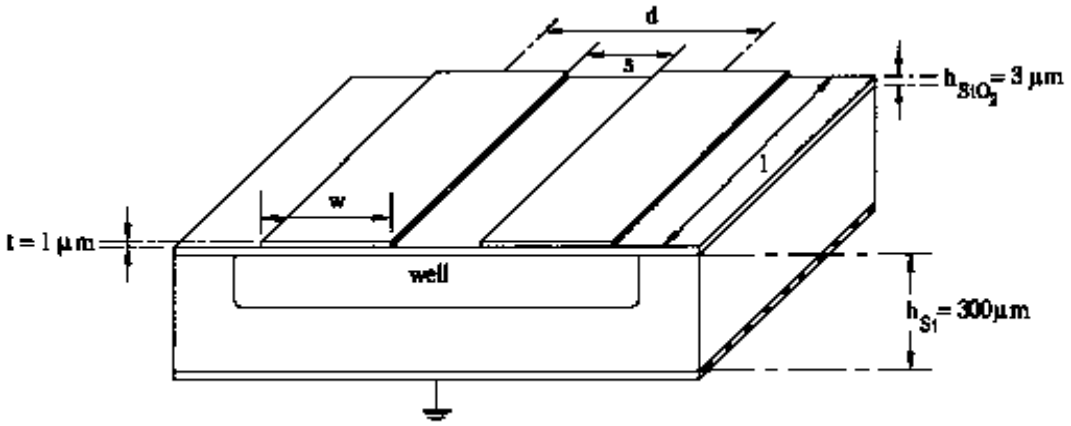

Fig.7a: Parallel coupled spiral segments over Si substrate.

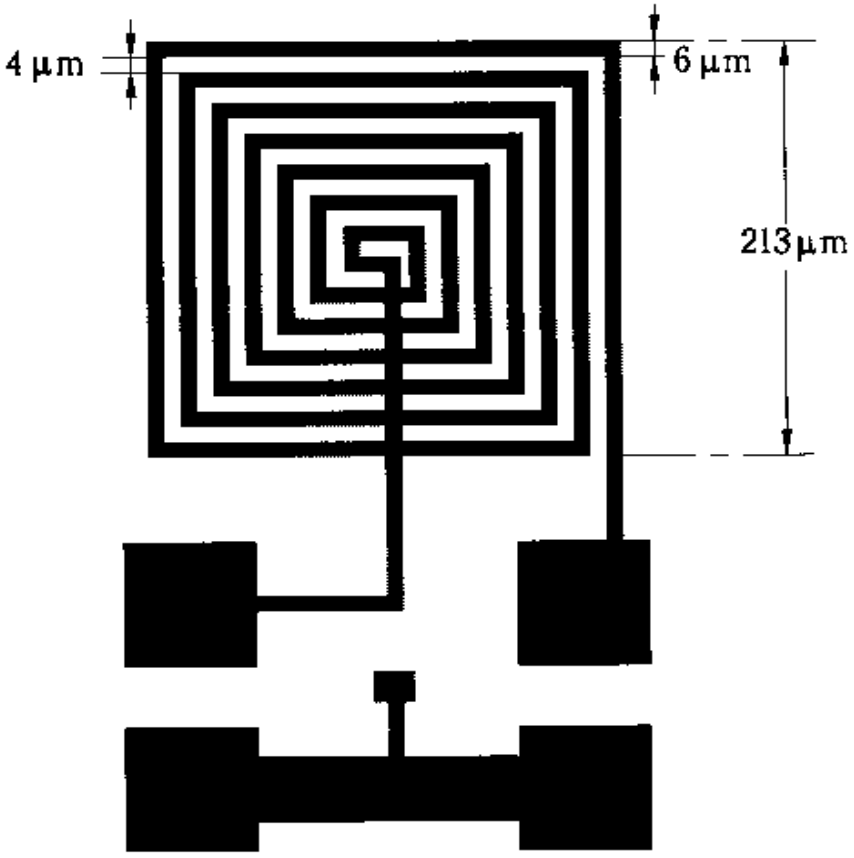

Fig.7b: Layout of Spiral inductor and probe pads for measurement.

The quality Q of this Spiral Inductor is changing as a function of frequency, which is shown in figure.8.

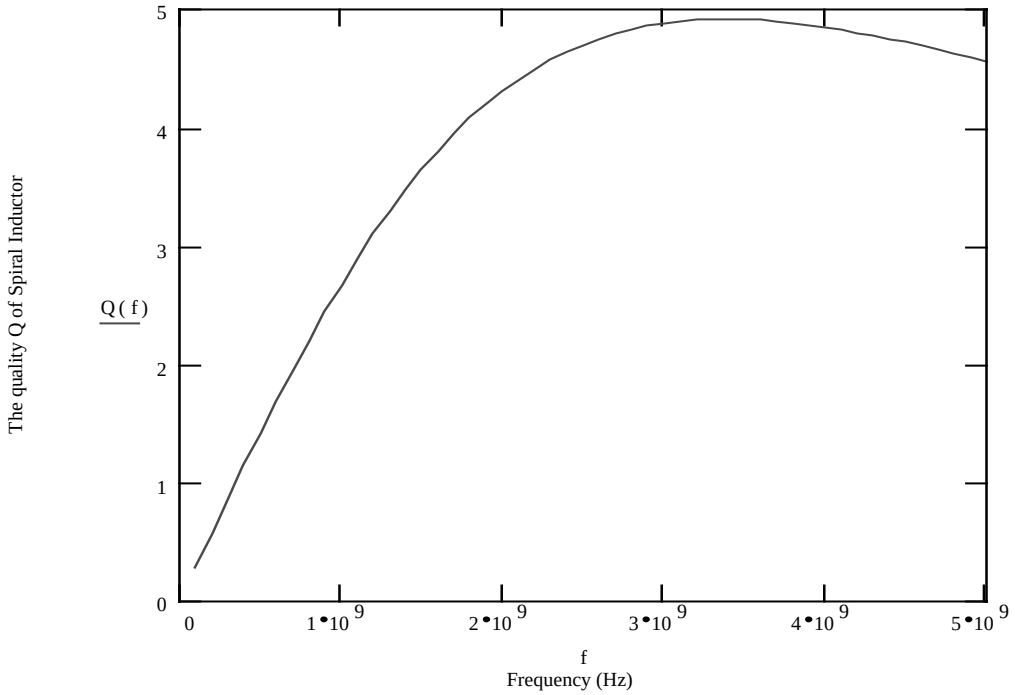

: Fig. 8: The quality Q factor of Spiral Inductor Vs frequency.

Figure 8 shows that the quality factor Q has the maximum value of 5 at frequency 3.2 GHz. At high frequencies, when the substrate impedance is smaller than the inductive impedance of the spiral, the substrate loss dominates and the Q is a decreasing function of frequency. That is why the plot of factor Q has a peak value. This is importance because the Spiral Inductor can be designed to have a peak Q at the frequency of interest.

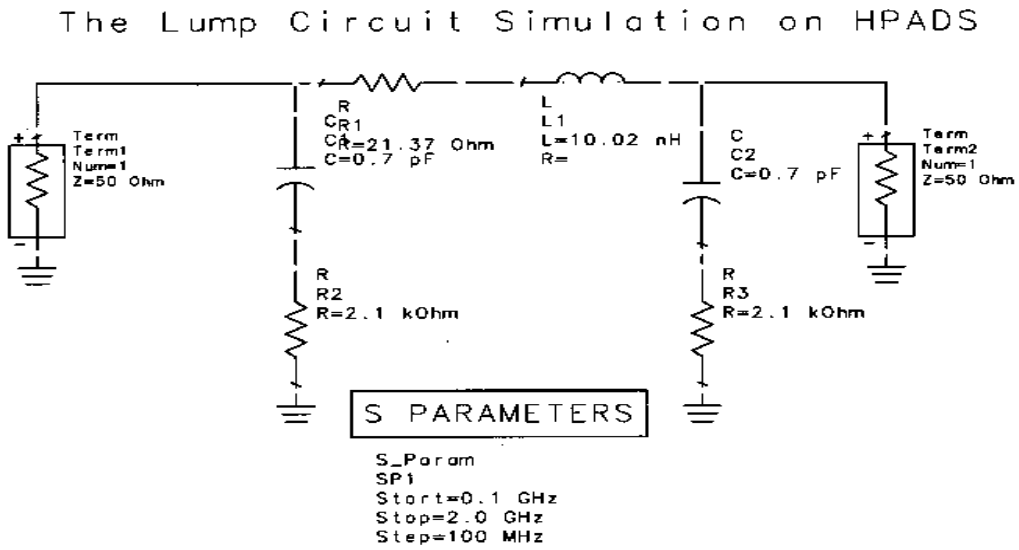

Fig. 8: Lump-circuit for simulation.

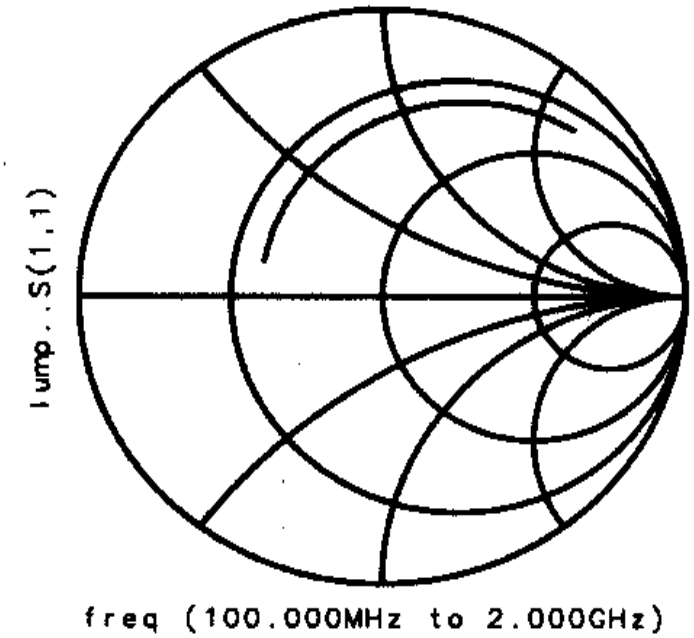

Fig.9: S_{11} parameter on Smith Chart

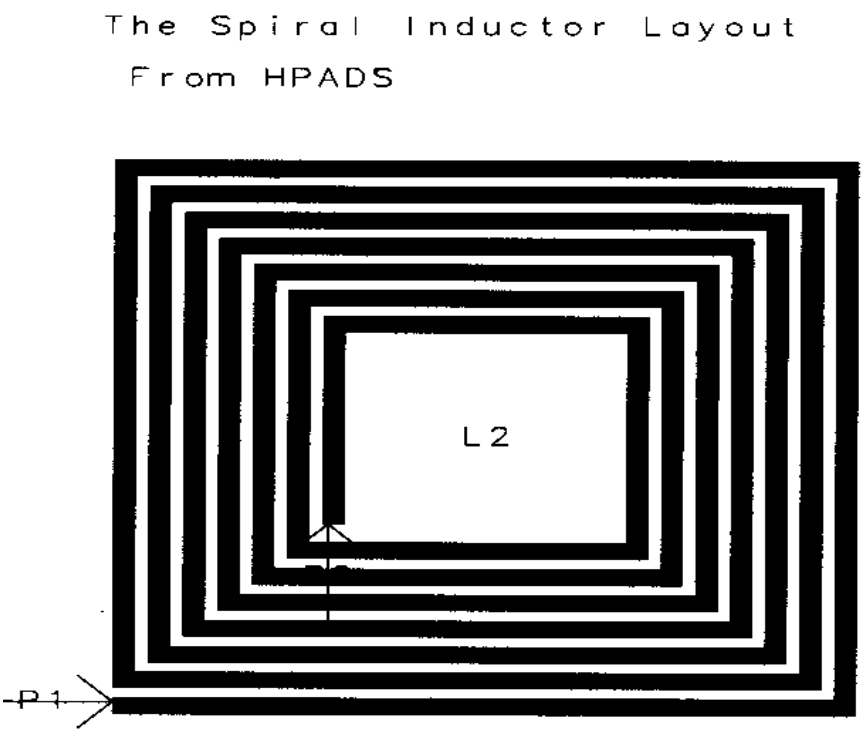

Fig.10. Spiral-inductor layout from HPADS program.

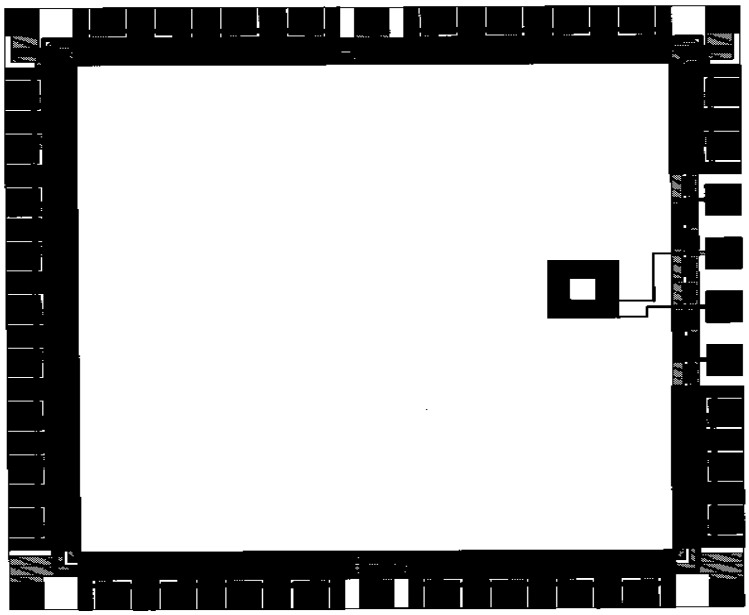

Fig.11: Spiral inductor on pad-frame of 2µ process.

4. Conclusion

This project is a challenge problem in practical design. Because the higher inductor value L_S, the smaller Quality value Q that the chip can be. This design has met all desired parameters but the quality of Q due to the loss in substrate and materials. This design can be optimized by Adding more turns and using smaller outer dimensions. Since the number of turns increases, the self- inductance and mutual inductance also increase, but the series resistance decreases, the DC loss can be reduced. Otherwise, at the high frequency, the substrate loss limits the Q, and the substrate capacitance lowers the self-resonant frequency of the structure. Clearly, utilizing thicker oxide and lower permittivity dielectric helps to reduce the capacitance. The substrate loss can be reduced by eliminating the substrate resistance. This can be done by either shorting out the substrate resistance or by opening circuit. Anyway, the main drawback of spiral inductors is their low Q when compared to air-wound coils occupying comparable circuit board area. Their main advantage are near zero cost, low tolerance value, excellent repeatability, good temperature performance, and low susceptibility to mechanical vibration.

References

1. N.M. Nguyen and R. G. Meyer, “ Si IC-compatible inductors and LC passive filter.” IEEE J. Solid-State Circuits, vol. 27, No. 10, pp.1028-1031, Aug.1990.

2. H. M. Greenhouse, “Design of Planar Rectangular Microelectronic Inductors”, IEEE Transactions On Parts, Hybrids, and Packaging, vol. PHP-10, No. 2, pp.101-109, June.1974.

3. L. Zu, Y. Lu, R. C. Frye, M. Y. Law, S. Chen, D. Kossiva, J. Lin, and K. L. Tai, “High Q-factor inductors integrated on MCM Si substrates.” IEEE Transactions on Components. Packaging and Manufacturing Technology, Part B: Advanced Packaging, Aug. 1996.

4. J. N. Burghartz, M. Soyuer, and K. Jenkins. “Microwave inductors and capacitors in standard multilevel interconnect silicon technology.” IEEE Trans. Microwave Theory Tech, vol. 44, No. 1, pp. 100-103, Jan. 1996.

5. J. R. Long and M. A. Copeland, “ The modeling, characterization, and design of monolithic inductors for silicon RF IC’s.” IEEE J. of Solid-State Circuits, vol. 32, No. 3, pp. 357-369, May. 1997.

射 频 和 天 线 设 计 培 训 课 程 推 荐

易迪拓培训(www.edatop.com)由数名来自于研发第一线的资深工程师发起成立，致力并专注于微波、射频、天线设计研发人才的培养；我们于 2006 年整合合并微波 EDA 网(www.mweda.com)，现已发展成为国内最大的微波射频和天线设计人才培养基地，成功推出多套微波射频以及天线设计经典培训课程和 ADS、HFSS 等专业软件使用培训课程，广受客户好评；并先后与人民邮电出版社、电子工业出版社合作出版了多本专业图书，帮助数万名工程师提升了专业技术能力。客户遍布中兴通讯、研通高频、埃威航电、国人通信等多家国内知名公司，以及台湾工业技术研究院、永业科技、全一电子等多家台湾地区企业。

易迪拓培训课程列表：http://www.edatop.com/peixun/rfe/129.html

射频工程师养成培训课程套装

该套装精选了射频专业基础培训课程、射频仿真设计培训课程和射频电路测量培训课程三个类别共 30 门视频培训课程和 3 本图书教材；旨在引领学员全面学习一个射频工程师需要熟悉、理解和掌握的专业知识和研发设计能力。通过套装的学习，能够让学员完全达到和胜任一个合格的射频工程师的要求…

课程网址：http://www.edatop.com/peixun/rfe/110.html

ADS 学习培训课程套装

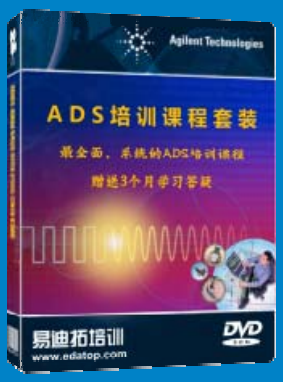

该套装是迄今国内最全面、最权威的 ADS 培训教程，共包含 10 门 ADS 学习培训课程。课程是由具有多年 ADS 使用经验的微波射频与通信系统设计领域资深专家讲解，并多结合设计实例，由浅入深、详细而又全面地讲解了 ADS 在微波射频电路设计、通信系统设计和电磁仿真设计方面的内容。能让您在最短的时间内学会使用 ADS，迅速提升个人技术能力，把 ADS 真正应用到实际研发工作中去，成为 ADS 设计专家...

课程网址： http://www.edatop.com/peixun/ads/13.html

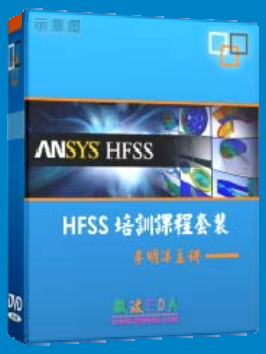

HFSS 学习培训课程套装

该套课程套装包含了本站全部 HFSS 培训课程，是迄今国内最全面、最专业的 HFSS 培训教程套装，可以帮助您从零开始，全面深入学习 HFSS 的各项功能和在多个方面的工程应用。购买套装，更可超值赠送 3 个月免费学习答疑，随时解答您学习过程中遇到的棘手问题，让您的 HFSS 学习更加轻松顺畅…

课程网址：http://www.edatop.com/peixun/hfss/11.html

CST 学习培训课程套装

该培训套装由易迪拓培训联合微波 EDA 网共同推出，是最全面、系统、专业的 CST 微波工作室培训课程套装，所有课程都由经验丰富的专家授课，视频教学，可以帮助您从零开始，全面系统地学习 CST 微波工作的各项功能及其在微波射频、天线设计等领域的设计应用。且购买该套装，还可超值赠送 3 个月免费学习答疑…

课程网址：http://www.edatop.com/peixun/cst/24.html

HFSS 天线设计培训课程套装

套装包含 6 门视频课程和 1 本图书，课程从基础讲起，内容由浅入深，理论介绍和实际操作讲解相结合，全面系统的讲解了 HFSS 天线设计的全过程。是国内最全面、最专业的 HFSS 天线设计课程，可以帮助您快速学习掌握如何使用 HFSS 设计天线，让天线设计不再难…

课程网址：http://www.edatop.com/peixun/hfss/122.html

13.56MHz NFC/RFID 线圈天线设计培训课程套装

套装包含 4 门视频培训课程，培训将 13.56MHz 线圈天线设计原理和仿真设计实践相结合，全面系统地讲解了 13.56MHz 线圈天线的工作原理、设计方法、设计考量以及使用 HFSS 和 CST 仿真分析线圈天线的具体操作，同时还介绍了 13.56MHz 线圈天线匹配电路的设计和调试。通过该套课程的学习，可以帮助您快速学习掌握 13.56MHz 线圈天线及其匹配电路的原理、设计和调试…

详情浏览：http://www.edatop.com/peixun/antenna/116.html

我们的课程优势：

※ 成立于 2004 年，10 多年丰富的行业经验，

※ 一直致力并专注于微波射频和天线设计工程师的培养，更了解该行业对人才的要求

※ 经验丰富的一线资深工程师讲授，结合实际工程案例，直观、实用、易学

联系我们：

※ 易迪拓培训官网：http://www.edatop.com

※ 微波 EDA 网：http://www.mweda.com

※ 官方淘宝店：http://shop36920890.taobao.com